

NJC

Accepted Manuscript



This is an *Accepted Manuscript*, which has been through the Royal Society of Chemistry peer review process and has been accepted for publication.

Accepted Manuscripts are published online shortly after acceptance, before technical editing, formatting and proof reading. Using this free service, authors can make their results available to the community, in citable form, before we publish the edited article. We will replace this *Accepted Manuscript* with the edited and formatted *Advance Article* as soon as it is available.

You can find more information about *Accepted Manuscripts* in the [Information for Authors](#).

Please note that technical editing may introduce minor changes to the text and/or graphics, which may alter content. The journal's standard [Terms & Conditions](#) and the [Ethical guidelines](#) still apply. In no event shall the Royal Society of Chemistry be held responsible for any errors or omissions in this *Accepted Manuscript* or any consequences arising from the use of any information it contains.

Cationic and anionic azo-dye removal from water by sulfonated graphene oxide nanosheets in Nafion membranes.

Silvia Scalese^{1,*}, Isabella Nicotera^{2,*}, Daniele D'Angelo¹, Simona Filice^{1,3}, Sebania Libertino¹, Cataldo Simari², Konstantinos Dimos⁴, Vittorio Privitera⁵

¹ CNR-IMM Zona Industriale Strada VIII n.5, I-95121 Catania, Italy

² Dipartimento di Chimica e Tecnologie Chimiche, Università della Calabria, via P. Bucci 14/D, I-87036 Rende (CS), Italy

³ Dipartimento di Scienze Chimiche, Università di Catania, viale A. Doria 6, 95125 Catania, Italy

⁴ Department of Materials Science & Engineering, University of Ioannina, GR-45110 Ioannina, Greece

⁵ CNR-IMM via Santa Sofia n.64 I-95123 Catania, Italy

Abstract

Graphene oxide flakes functionalized with 3-amino-1-propanesulfonic acid (denoted as GO_{SULF}) as powder or incorporated into an ionomer membrane such as Nafion (DuPont) were studied for water purification applications. The adsorption and the photocatalytic activity of GO_{SULF} powder itself or confined as nano-additive in the membrane (Nafion-GO_{SULF}) were investigated by measuring the degradation of a cationic dye, methylene blue (MB), in dark and under UV/visible light illumination. The results were compared with the ability of these systems to degrade an anionic dye, methyl orange (MO), in order to evaluate the role of polymer-dye interaction. The degradation of the azo dyes depends on the mutual interaction between GO_{SULF} flakes, the polymeric matrix and the dye: Nafion-GO_{SULF} strongly reduces MB both in dark and illumination condition in the same way of the GO_{SULF} powder, while, for MO degradation, the composite membrane is more efficient than GO_{SULF} alone. Finally, the possibility to reuse the same photocatalytic material several times, that is the main advantage of embedding active nanomaterials in a polymer matrix, is demonstrated by effective regeneration of the nanocomposite membranes.

Keywords: Nafion, graphene oxide, functionalization, dye adsorption, photocatalysis.

*Corresponding authors:

e-mail (S. Scalese): silvia.scalese@imm.cnr.it;

e-mail (I. Nicotera): isabella.nicotera@unical.it

Introduction

The use of nanotechnology for water purification applications has attracted an increasing interest in the last decade. The development of new, efficient, eco-friendly and specific methods to treat contaminated waters is of fundamental importance due to the increase of pollution mainly coming from industrial sites¹⁻⁵.

Among a long variety of chemical pollutants, the effluent streams coming from textile plants must be treated in order to remove the toxic or carcinogenic dye residues and their by-products, that otherwise could be released in the environment^{3,6}. In particular, azo dyes constitute about 50% of dye normally used in textile industries. Many technologies have been developed for dye removal from aquatic environments, including physical, chemical, and even biological approaches⁷⁻⁸. Among these approaches, absorption is regarded as an easy and economic process⁹⁻¹⁰. Various materials, such as commercial activated carbon, natural materials, bio-adsorbents and wastes from agriculture have been used for such processes⁹⁻¹⁰.

Carbon-based nanomaterials have been used as high capacity and selective sorbents for organic solutes in aqueous solutions¹¹, or in combination with other nanomaterials to increase the photocatalytic activity of these nanomaterials in water purification, energy conversion, etc.^{12,13,14,15}. In particular, graphene oxide (GO), composed of graphene flakes with oxygen functional groups on the basal planes and at the edges¹⁶, can be used as precursor of graphene for the synthesis of graphene-based semiconductors¹⁷ or it can be directly used as an effective absorbent for methylene blue (MB), which is widely applied to dye cotton, wood and silk. The huge and fast MB absorption capacity¹⁸ of GO flakes makes this material very competitive with other high performance absorbents.

Recently, photocatalytic properties have been reported for GO¹⁹ due to the creation of highly reactive species in water (hydroxyl radical or oxygen ions) induced by light absorption and capable to remove organic contaminants. GO is also used as starting materials for the preparation of graphene-based composite photocatalysts used in many reactions, such as nitroaromatics reduction, alcohols oxidation, CO₂ reduction, in water splitting application, disinfection and elimination of water pollutants^{20,21}. In particular, reduced GO (rGO) and rGO-TiO₂ composites have been tested to remove cationic dye such as MB from water by simple adsorption phenomena²². In addition, recently sulfonated graphene has been mostly used as catalyst for esterifications, Friedele Crafts reactions and biomass transformation²³. Recent studies also suggested that sulfonated graphene (GR-SO₃H) can enter in the production of electrodes for the next generation of high performance electrochemical capacitor and can be crosslinked with hierarchical mesoporous TiO₂ for the

fabrication of membranes used for water purification²³. The versatile properties of these sulfonated materials can be attributed, at least in part, to the peculiar structure of graphene, consisting of a honeycomb-structured two-dimensional sheet of sp^2 -hybridized carbon having one-atomic thickness, and to the fact that GR-SO₃H displays Brønsted acid properties²³.

In general, the main disadvantage of using nanomaterials for water purification is that they are dispersed as powder in water and a powder itself could be a contaminant for the environment and, furthermore, cannot be easily reused. The combined use of membrane technology and nanomaterials is expected to overcome these problems. In particular, carbon nanomaterial are providing novel opportunities to develop more efficient reactive membranes for the removal of water pollutants. In previous works²⁴⁻²⁵ we have already shown the promising use of Nafion® (DuPont) polymer for producing nanocomposite membrane (containing GO or TiO₂) for water purification applications. In particular these nanocomposites were tested for the removal of methyl orange and methylene blue from aqueous solution.

In this work, we prepared organo-modified GO containing sulfonic functional groups (GO_{SULF}), by reaction with an acidic amine derivative covalently bonded to the graphite surfaces via nucleophilic substitution reactions on the epoxy groups of GO (see Fig.1)²⁶.

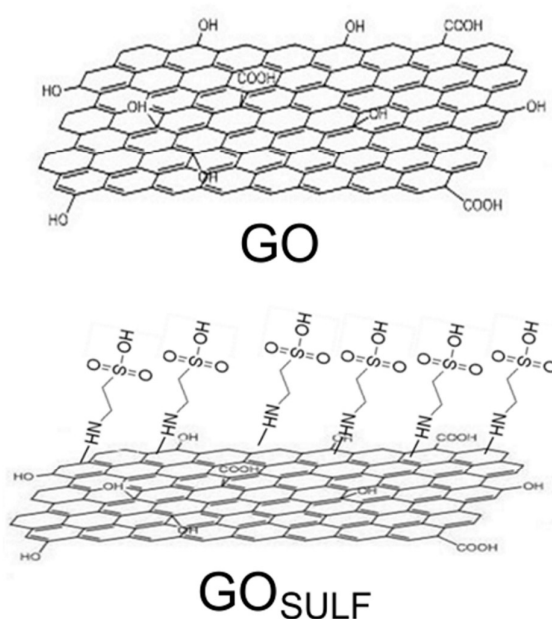


Fig.1: Schematic representation of the structures of GO (top) and GO_{SULF} nanosheet (bottom).

GO_{SULF} was then dispersed into an ionomer, such as Nafion, in order to create nanocomposite membranes. Nafion® (DuPont) is a perfluorosulfonic polymer that shows significant properties

such as high ionic conductivity, ion-exchange capacity and stable structure, therefore it is used for various applications such as fuel cells, sensors, electrochemical devices²⁷⁻²⁸.

The choice of this ionomer for the creation of hybrid films to be tested in applications for the purification of the water is substantially linked to two reasons: 1) the acidic properties promote the separation of ionic compounds present in the water; 2) the Nafion membranes have a high capacity to absorb water favouring the effective interactions between contaminants and the active material²⁴. The organo-functionalization of the GO surfaces with hydrophilic groups such as $-\text{SO}_3\text{H}$, improve both the acidity and the water uptake of the resulting nanocomposite membranes, but also their mechanical, chemical, and thermal strength²⁶.

Recent results show for GO_{SULF} nanosheets a better absorption capability in the removal of MB with respect to the GO powder²⁹. In this work, the degradation ability of GO and GO_{SULF} flakes for removing methylene blue (MB) molecules from water in dark and under UVA/Blue illumination was investigated and compared. Following, our study was focused on the Nafion- GO_{SULF} composite membrane in the removal of both MB and methyl orange (MO) (the structural formulae of these two molecules are reported in Fig.2), which differ for their superficial charge.

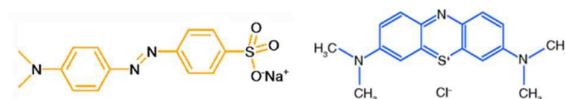


Fig.2: Structure of methyl orange (left) and methylene blue (right).

The degradation mechanism involves both adsorption and photocatalytic processes, and the results point out as such hybrid nanocomposites are effective for the selective removal of different azo dyes. In this mechanism the polymer matrix seems to play a crucial role and synergic with the nano-additive. Finally, the possibility of regeneration and reuse of the Nafion- GO_{SULF} composite was also tested in order to demonstrate as the incorporation of nanomaterials inside a polymeric film is a more efficient and ecologically friendly method with respect to the direct dispersion of powders in aqueous solution.

Experimental

Methylene blue (0.1 M in H_2O) and methyl orange (0.1 wt% in H_2O) were acquired from Sigma-Aldrich. Nafion as a 20 wt% dispersion in water and lower aliphatic alcohols was supplied by Aldrich. GO_{SULF} was obtained by treating GO prepared by the Staudenmaier's method³⁰ with 3-

amino-1-propanesulfonic acid, as described in a previous work²⁶. With respect to the synthesis of sulfonated graphene reported in the literature²³ in which the sulfonic group is linked on the graphene layer by a phenyl ring, in our work the modification of graphene oxide occurs by the replacement of epoxy functionalities by amine derivatives ending with a sulfonic group. The result is schematically reported in Fig.1. This reaction occurs without the formation of intermediate products that should be isolated and purified by filtration and centrifugation, as in the case of the synthesis reported in literature. In a previous work²⁶ Fourier Transform infra-red (FT-IR) spectroscopy performed on GO_{SULF} showed the reduction of the epoxy groups along with the appearance of the signals related to CH₂ on amine groups; TGA/DTA analysis confirmed a 22% functionalization of graphene oxide epoxy functionalization with the amine derivative.

X-ray photoelectron spectroscopy (XPS) measurements were performed under ultrahigh vacuum conditions with a base pressure of 5×10^{-10} mbar in a SPECS GmbH instrument equipped with a monochromatic MgK α source ($h\nu = 1253.6$ eV) and a Phoibos-100 hemispherical analyzer. All binding energies were referenced to the C1s core level at 284.6 eV. Spectral analysis included a Shirley background subtraction and peak deconvolution employing mixed Gaussian–Lorentzian functions, in a least squares curve-fitting program (WinSpec) developed at the Laboratoire Interdisciplinaire de Spectroscopie Electronique, University of Namur, Belgium.

Field emission scanning electron microscope (Zeiss Supra35 FE-SEM) was used to observe the morphology of the samples. Cross SEM analysis was carried out on the section of the membranes broken in two parts after freezing by immersion in liquid nitrogen.

Nafion and Nafion-GO_{SULF} composite membranes were prepared by a solvent casting method as described in previous works²⁴⁻²⁶. The composite was prepared with 3 wt% filler-to-polymer loading. All the membranes produced were subsequently acid-activated by rinsing in: (i) boiling HNO₃ solution (1 M) for 1 h to oxidize the organic impurities, (ii) boiling H₂O₂ (3 vol %) for 1 h in order to remove all the organic impurities, (iii) boiling deionized H₂O for 40 min three times, (iv) boiling H₂SO₄ (0.5 M) for 1 h to remove any metallic impurities, and again (v) boiling deionized H₂O for 40 min twice to remove excess acid.

Regeneration process of the membranes after the adsorption experiments was performed by boiling them in acid water (1% of nitric acid in deionised water) for about 30 min, until the membranes return to their initial colour as a consequence of the release of the adsorbed dye molecules. Then, the membranes were rinsed again in boiling acid water for 15 minutes and, finally, twice in boiling water for 15 min, respectively. Membranes were dried at 100 °C on a hot plate for 180 min and weighed before each adsorption test.

The surface charge of sulphonated graphene oxide and graphene oxide solutions was measured

using an Horiba Scientific NanoParticle Analyzer SZ-100-Z. The results show that at pH = 6.3 both materials are negatively charged, confirming the literature data³¹. In particular, the zeta potential of GO is higher (-46 mV) than the zeta potential of GOSULF (-42.8 mV).

The adsorption ability of GO_{SULF} powder directly dispersed in MB solutions at different concentrations (10, 70 and 100 mg/l) was evaluated by measuring the decrease of MB concentration.

The photocatalytic activity of GO_{SULF} powder and membranes was evaluated by measuring the degradation of MO and MB in water solution with an initial concentration of $1.5 \cdot 10^{-5}$ M under UV-Vis light irradiation carried out with a 18W UVA/blue DULUX OSRAM lamp. In the case of membranes, the photocatalytic experiment was performed by dipping one piece of about 1 cm² into 2 ml of dye solutions. The solutions were analysed by recording variations of the absorbance spectra of dyes using an UV/Vis AGILENT Cary 50 spectrophotometer in a wavelength range between 200 and 800 nm and wide optical window cuvettes (200-2500 nm). The degradation of dyes was evaluated by the Lambert-Beer law via the absorbance peak at 465 nm and 664 nm for MO and MB, respectively. Dye adsorption (in dark conditions) for each membrane was also evaluated in order to discriminate between the contributions of the mere adsorption and the photocatalytic activity. The absorption of MB dye was also tested by varying the size of the membrane piece.

Dye solution pH was measured by a Mettler Toledo SevenGO duo SG23 pH-meter. The water content value of each membrane was determined using a microbalance and recorded as: uptake% = $[(m_{\text{wet}} - m_{\text{dry}})/m_{\text{dry}}] \times 100$, where, m_{dry} is the mass of membrane dried in oven at 60 °C for 2 h and then put to equilibrate in a desiccator before being weighted; m_{wet} is the weight of the membrane after immersion in distilled water at room temperature for at least 48 h and quickly blotted dry with a paper tissue in order to eliminate most of the free surface liquid.

Results and discussion

XPS and SEM characterization

The C1s core level X-ray photoemission spectra of starting GO and sulfonated GO are shown in Figs. 3a and b.

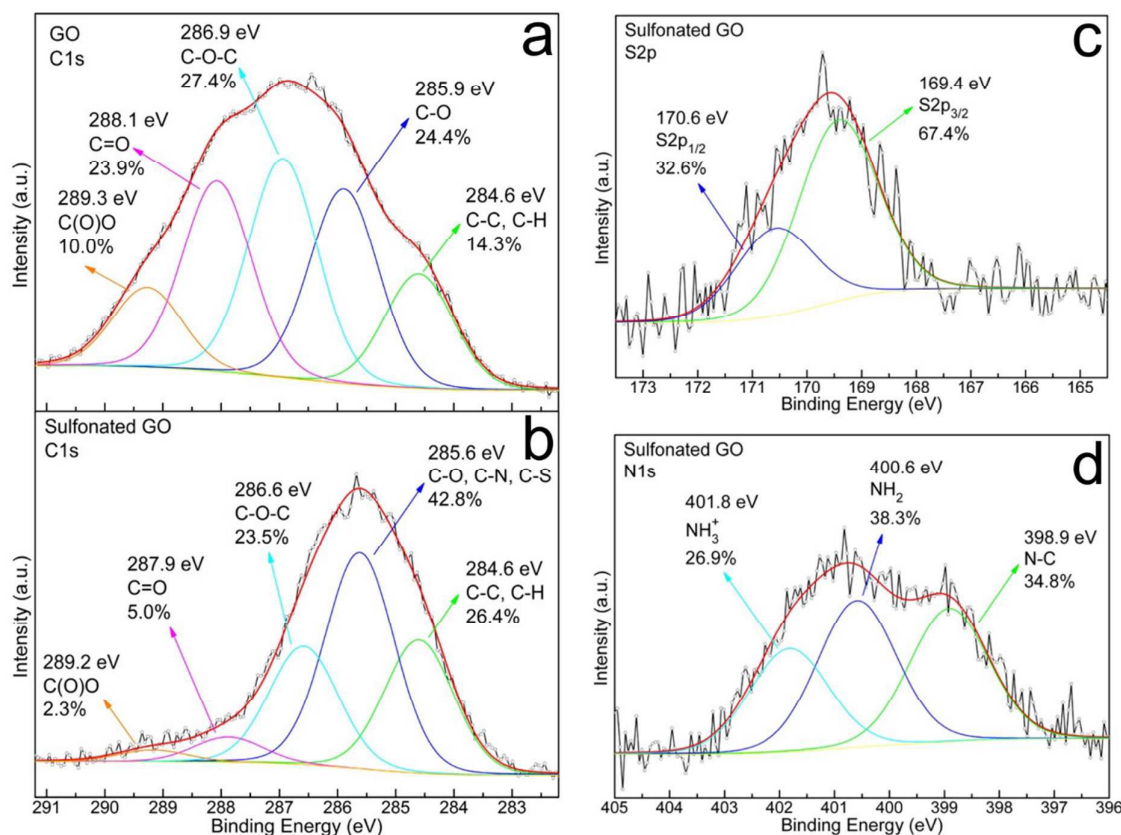


Fig. 3: X-ray photoemission spectra of (a) C1s core level for starting GO and (b) C1s, (c) S2p and (d) N1s for sulfonated GO.

After deconvolution with mixed Gaussian–Lorentzian functions both spectra consist of five components. The first peak at 284.6 eV is attributed to the C-C/C-H bonds, while the second at ~285.6–285.9 eV is assigned either to C-O bonds in the case of starting GO or to C-O and C-N/C-S bonds for the sulfonated GO. Following bands at higher binding energies (i.e. ~286.6–286.9 eV, ~287.9–288.1 eV and ~289.2–289.3 eV) are ascribed to C-O-C, C=O and C(O)O groups in that order³². Comparison of the two C1s XPS spectra suggests the successful sulfonation of GO as the contribution to the total C1s integrated intensity of the first two peaks is significantly enhanced upon sulfonation. Specifically and as expected, the incorporation of 3-amino-1-propanesulfonate leads to the insertion of additional C-C, C-H, C-N and C-S bonds and thus we observe a 26.4% contribution for C-C/C-H and 42.8% for C-O/C-N/C-S, in contrast to the relevant percentages, 14.3% and 24.4%, of the starting GO.

These findings are verified by the detection of nitrogen and sulphur in the case of sulfonated GO (Figs. 3c and d). Three dominant signals are revealed in the N1s binding energy window upon fitting with an admixture of Gaussian–Lorentzian functions. All three originate from 3-amino-1-propanesulfonate and are correlated with C-N and N-H bonds of protonated or not amines³³.

Furthermore, a sulphur species is exposed at a high binding energy in the S2p region. The latter is associated with highly oxidized sulphur groups, i.e. sulfonates^{34,35}. The aforementioned data along with the fact that no nitrogen and sulphur were detected in the starting GO sample conclude that XPS results clearly demonstrate the successful GO sulfonation.

Figures 4a and 4b show the cross-sectional SEM images of Nafion and Nafion-GO_{SULF} membranes, respectively. GO_{SULF} sheets appear to be homogeneously distributed throughout all the membrane thickness. In our previous work²⁴, the EDX analyses of the cross section of Nafion-GO_{SULF} were added as supplementary information to confirm the homogeneous dispersion of nanomaterial inside the polymeric matrix. GO_{SULF} powder has been dispersed on a silicon substrate by drop-casting and SEM images at two different magnifications show both well dispersed GO sheets (dark regions) and GO aggregates on the Si substrate, as reported in Fig.4c.

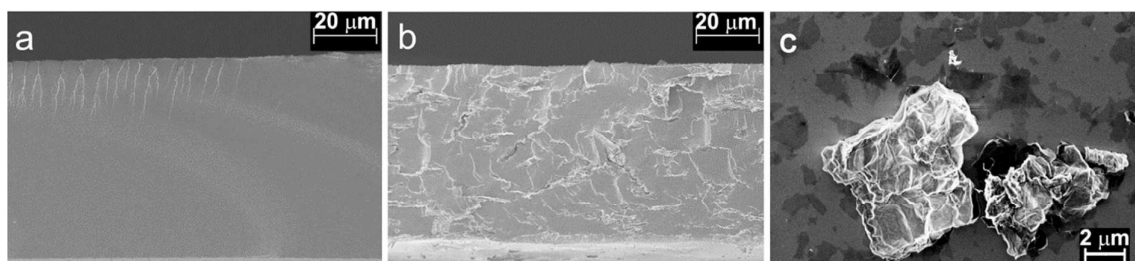


Fig. 4: Cross-sectional SEM images of (a) Nafion membrane and (b) Nafion-GO_{SULF} membrane loaded with 3% of GO_{SULF}; (c) GO_{SULF} powder dispersed on a Si substrate.

Removal of methylene blue

The degradation of MO and MB dye-molecules arising from contact with GO_{SULF} powder and Nafion-GO_{SULF} membrane has been investigated. The membrane sheets used in this experiment have area of 1cm² and thickness of about 60 μm. In order to compare the degradation results both through powder and through membrane, the mass weight of GO_{SULF} powder dispersed in 2 ml of dye solutions is exactly the same amount loaded in 1 cm² membrane, i.e. 70 μg/ml. We have chosen MO and MB as model compound for the photocatalytic study, since azo-dyes constitute one of the most diffuse water contaminants. In particular, these two dyes differ for the sign of their superficial charge (Scheme 2) allowing to investigate the charge effect on their adsorption and degradation by the polymeric matrix.

MB is a cationic, thiazine dye, which absorbs light in a band centred at 664 nm (n-δ*) (monomer) with a shoulder at 610 nm corresponding to the MB dimer³⁶. The first absorbance peak was used to quantify the MB concentration reduction or degradation due to adsorption and

photocatalysis. Figure 5 shows the absorbance spectra of MB solution containing different concentrations of GO_{SULF} powder (10, 70 and 100 mg/l).

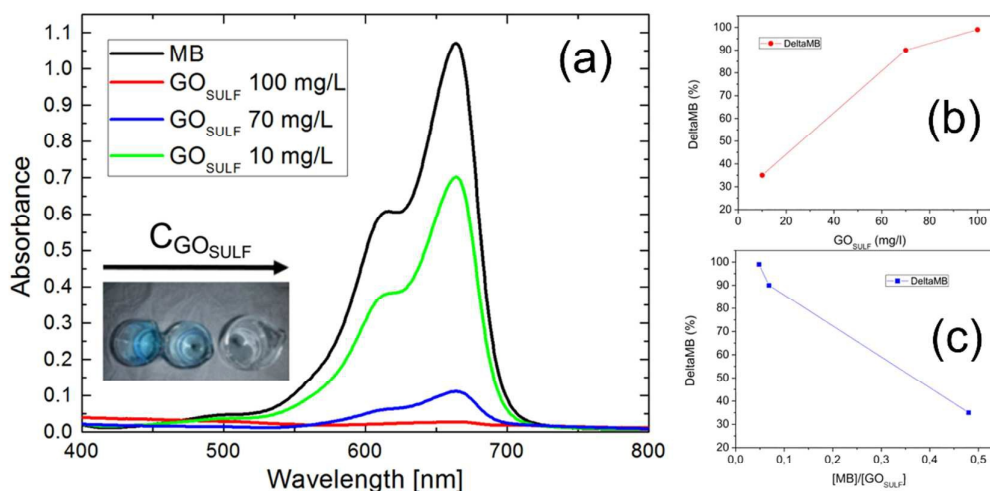


Fig. 5: (a) UV-Vis absorbance spectra of MB solution after adding GO_{SULF} powder with different concentrations: 10 mg/l (green curve) 70 mg/l (blue curve) and 100 mg/l (red curve). The initial absorbance of the MB is also reported (black curve). The photo in the inset shows the beakers containing the MB solutions with GO_{SULF} with increasing concentration (from left to the right). In (b) and (c) the removed MB (%) as a function of GO_{SULF} concentration or as a function of the $[\text{MB}]/[\text{GO}_{\text{SULF}}]$ concentration ratio are reported, respectively. The lines in the plots are just a guide for the eye.

The presence of GO_{SULF} powder significantly reduces the MB concentration in the dark. This likely is related to the dye positive superficial charge that favours its adsorption on GO_{SULF} surface through electrostatic interactions with the negative charge of sulfonic groups. The removal of MB increases with powder concentration and occurs immediately in the first minutes, causing the formation of MB- GO_{SULF} precipitates at the bottom of the beaker (see the inset photos of Fig.5). The addition of a larger amount of GO_{SULF} allows to remove MB from water more effectively and rapidly. A 35% decrease of MB due to adsorption is observed for a GO_{SULF} content of 10 mg/l. By increasing the GO_{SULF} concentration in solution of one order of magnitude (100 mg/l), the residual MB reduces down to ~1% of the initial value. An important factor affecting the adsorption is the ratio between dye and GO_{SULF} concentrations. In our case the MB concentration is 4.8 mg/l and is comparable with the lower GO_{SULF} concentration here considered (10 mg/l). In Figs.5(b) and (c) we report the removed amount (%) of the dye as a function of GO_{SULF} concentration or as a function of the MB/ GO_{SULF} concentration ratio. The trend in the graph in Fig.5b is linear only in a limited region, where the two concentrations are comparable, then it seems to reach a plateau value; the plot

reported in Fig.5c suggests that the range $[MB]/[GO_{SULF}]$ between 0.1 and 0.5 should be further studied in order to investigate the linearity of the trend.

The GO_{SULF} powder was also tested as photocatalyst under UV-blue light irradiation. We have tested the photostability on GO and GO_{SULF} in water, without the presence of the dye, within the experimental irradiation conditions used in this work, and we observed no evident variation in the UV-Vis absorbance spectra. As explained in the introduction, recently a photocatalytic activity has been observed for GO and this was shown to depend on the oxygen quantity bound on graphene layers¹⁹. Clearly, it is expected that the functionalization of graphene oxide surface by, for example, the grafting of amine derivatives (as in this case) can change its photocatalytic activity. In Figure 6 we compare the residual concentration of MB as a function of dipping time with GO_{SULF} and GO powders (70 mg/l).

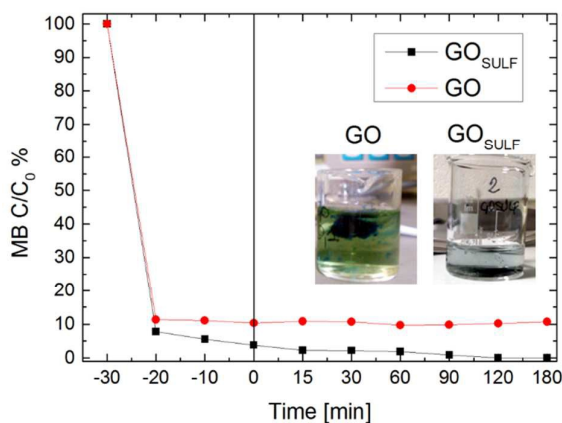


Fig.6: MB residual concentration versus time of contact with GO and GO_{SULF} powders (both with a concentration of 70 mg/l). The UV-blue lamp irradiation starts after 30 min of adsorption in dark, as indicated by the vertical line at $t = 0$ min. Lines in figure are guides for the eyes. The photos in the inset show the beakers containing the MB solutions with GO_{SULF} and GO after 10 min adsorption ($t = -20$)

After 30 minutes of adsorption in dark, the solution is exposed to UV-blue light irradiation up to three hours. The time zero indicates the starting of UV-blue irradiation. The adsorption takes place immediately for both the powders and is more efficient for GO_{SULF} than for GO, even though the loss of O groups due to sulfonic functionalization (confirmed by XPS measurements) makes GO_{SULF} less negative than GO, as shown by zeta-potential measurements. This can be explained by considering also the structural differences between the two kinds of GO observed by XRD analysis²⁶: the sulfonic functionalization induces a larger distance between GO planes and, therefore, the accessibility of the active sites to the dye molecules in the two GO materials is different. The adsorption on GO layers occurs immediately with the formation of aggregates depending on the oxygen moieties on the graphene layers and MB-GO flocculates appear in the

solution, as explained in ref 22. On the contrary, when the epoxy functionalities on the graphene layers are substituted by organo-amine ending with acid groups, the MB aggregation does not occur, but immediately MB-GO_{SULF} precipitates at the bottom of the beaker.

MB-GO aggregation is clearly evidenced by the appearance of a peak at 577 nm²², which instead is not observed for GO_{SULF} (see Fig. 5). In addition, GO_{SULF} shows a slightly further MB decrease when irradiation starts, after 30 minutes of absorption in dark, while in GO the MB concentration reaches the minimum value after 10 min in dark and then there is not further reduction either with time or during irradiation. In the absence of photocatalysts we have not observed any degradation of MB under UVA/blue irradiation for the same irradiation time. Since the main removal effect is due to adsorption that reduces drastically the initial MB concentration, the photocatalytic activity of the powders has not been further investigated within these experimental conditions in this paper.

However, the use of photocatalytic powders directly dispersed in solution for the contaminants removing is not advisable for two main issues: i) the removal of these powders from the water at the end of the process and ii) the possibility to reuse them.

In this study, we tested the activity of the photocatalytic material incorporated inside a polymeric membrane, through the creation of a nanocomposite which prevents its release. A comparison among the activities of the materials directly dispersed in water or embedded in a polymeric membrane is reported in the following discussion. In order to understand the role of the polymeric matrix in dye degradation, the results obtained for MB were compared with those obtained for the removal of an anionic dye, methyl orange (MO), as explained later on.

Figure 7 compares the residual MB concentration of aqueous solutions in contact with Nafion and Nafion-GO_{SULF} membranes, both in dark and under UV-blue irradiation. Nafion itself can easily adsorb MB²⁴.

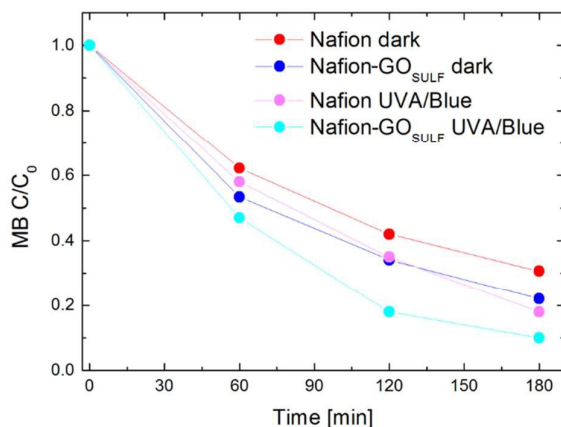


Fig.7: MB residual concentration versus time of contact with Nafion and Nafion-GO_{SULF} in dark (red and blue

dots, respectively) and under irradiation (magenta and cyan dots, respectively).

The ability of these membranes in the degradation of the azo dyes depends mainly on the mutual interaction between the dye and the Nafion polymer³⁷. Nafion is a proton exchange membrane thanks to the sulfonic groups (SO_3H) on the side chains, and responsible for its high proton conductivity. Cationic molecules, such as MB dye, are strongly affected by electrostatic attraction from the SO_3^- groups in Nafion, and ion exchange in the hydrophilic sites of the membrane can be achieved. Consequently, Nafion- GO_{SULF} composite shows better performance than filler-free Nafion membrane, both in dark and under illumination, since the nano-dispersion of the filler inside the polymeric matrix increases the number of acid sites in the electrolyte (SO_3^-) for adsorption and also its water uptake and proton conductivity²⁶.

Figure 8 reports the MB residual concentration after Nafion- GO_{SULF} membranes with different size (0.25 , 0.50 and 1.00 cm^2) were immersed in the solution in dark of as a function of time (until 5 hours).

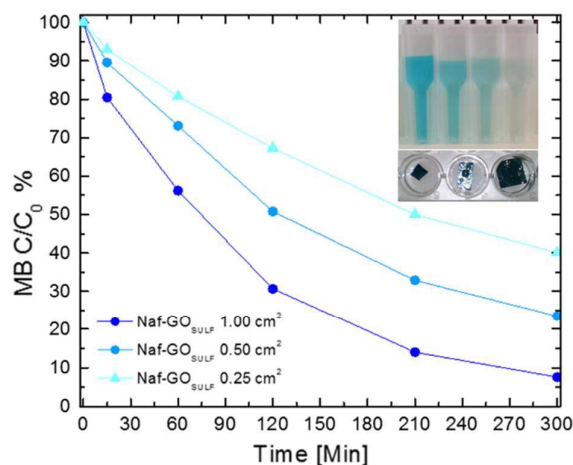


Fig.8: MB residual concentration versus contact time in dark with Nafion- GO_{SULF} membranes having different surface areas. In the inset we report the pictures of the membranes used for MB adsorption (from left to right: 0.25 cm^2 , 0.5 cm^2 , 1 cm^2) and the cuvettes with initial MB solution (first on the left) and solutions after dipping the three Nafion- GO_{SULF} membranes for 5 hours.

The adsorption increases proportionally to the membrane area as a consequence of the variation of the number of active sites. The figure also reports the pictures of the cuvettes filled with the MB solutions (from left to right: MB initial concentration and after immersing a 0.25 cm^2 , a 0.5 cm^2 and a 1 cm^2 membrane respectively) and the corresponding membranes after the experiment. Clearly, for the same volume and MB concentration, a membrane with larger area induces a more significant decolourization effect.

Another aspect to be considered in this analysis is related to the capacity of a membrane to absorb water. In fact, the water absorption on polymer surface favours the interaction of electrons and holes with water molecules or hydroxyl ions, forming reactive species that are able to degrade organic compounds³⁸. As reported elsewhere^{26,39}, Nafion-GO_{SULF} composite membrane is much more hydrophilic with respect to filler-free Nafion, showing a water uptake value doubled, i.e. about 50 wt% and about 24 wt%, respectively. This so high hydrophilicity of the composite can be addressed as the main cause of its better dye removal ability both as adsorbent and under irradiation.

Comparing the results of Figs. 6 and 7, the degradation of MB is larger when GO_{SULF} is directly dispersed in dye solution with respect to the case of GO_{SULF} embedded in the polymeric matrix. The MB adsorption by the GO_{SULF} occurs immediately and it is larger in comparison with the adsorption capacity of Nafion-GO_{SULF}; it is also known that adsorption of dyes on the surface of photocatalytic material is needed in order to achieve dye degradation⁴⁰. The adsorption on GO_{SULF} nanoparticles is favoured respect to the adsorption on Nafion nanocomposite since in the former case the active sites are immediately accessible to MB molecule while in the latter case the MB molecules have to diffuse inside the polymeric matrix. Nevertheless, the powder incorporation inside a polymeric matrix gives the advantage to overcome the problems related to the recovery of materials at the end of the process and nanocomposite Nafion membranes can be reused for several purification processes.

Removal of methyl orange

The role of polymeric matrix in the degradation ability of organo-modified graphene oxide is discussed below comparing the results obtained for MB with the ones obtained for MO. As discussed before, in the latter case the interaction between the dye and the composite (both Nafion polymer and nano-additive) is not favoured due to electrostatic repulsion.

Figs.9a and 9b report the absorbance spectra of MO solution obtained after dipping Nafion membrane, Nafion-GO_{SULF} membrane and GO_{SULF} powder for one hour in dark and under UVA/blue irradiation, respectively.

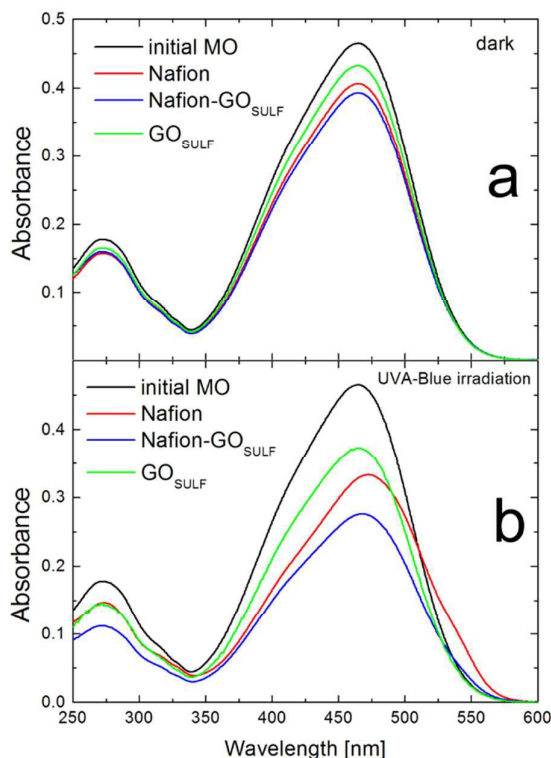


Fig.9: UV–Vis absorbance spectra of methyl orange after immersing Nafion (red curves), Nafion- GO_{SULF} (blue curves) composite membranes and GO_{SULF} powder (green curves) in MO solution for one hour in dark (a) or under UV/blue irradiation (b).

The UV/Vis absorbance spectrum of MO dissolved in water shows two maxima: the first at 270 nm and the second at 465 nm. The absorbance at 270 nm is assigned to the benzene ring in MO, whereas the absorbance at 465 nm is due to the azo linkage of MO⁴¹. The latter absorbance peak was used to quantify the MO concentration reduction or degradation due to adsorption and photocatalysis; any variation of the 270 nm peak position is correlated to the formation of by-products as a consequence of the azo-dye photodegradation. No degradation of MO under UVA/blue irradiation for 1 h has been observed in the absence of photocatalysts (membranes or powder)²⁴.

MO adsorption, clearly, is quite small for all the materials, whereas the irradiation induces a significant decrease of the dye, in particular in the case of Nafion- GO_{SULF} . As explained in our previous work²⁴, MO is an anionic dye molecule, so its adsorption on Nafion based composite membranes is hindered because of the electrostatic repulsions between the negative molecular charge of the dye and the negative charge of sulfonic groups in Nafion. The effect of MO

adsorption on GO_{SULF} powder in dark conditions consists of a small reduction of the initial dye concentration (6.5%) and this reduction rises to 15.6 % in presence of the polymer.

GO can work as a photocatalyst for water decomposition¹⁹, and that different oxygen functionalities (in our case an amine-derivative functionality replaces oxygen atoms) can modify the valence band and conduction band positions.

Under UV/Vis light irradiation, the decrease of MO is larger with respect to the absorption in dark (Fig. 9b). In the case of Nafion membrane a small shift towards larger wavelength is observed, due to the protonation of MO^{42} . In fact, a reduction of the pH of the solution is recorded due to the release of protons from the acid membrane to the solution when the dye is adsorbed. As we have seen, the best performance is achieved by using the Nafion- GO_{SULF} composite membrane because with respect to filler free Nafion membrane, the nano-additive increases the acidity and the water uptake capacity of the polymer film.

Under irradiation, the initial MO concentration (Figure 9b) decreases and reaches the final value of 55% in the presence of Nafion- GO_{SULF} and 82% for GO_{SULF} . No toxic by-products, as for known photocatalyst like TiO_2 ⁴³, are formed: the decrease of MO concentration by Nafion- GO_{SULF} is due to adsorption of the MO molecules favoured by irradiation. Therefore, the use of Nafion- GO_{SULF} membrane for MO dye removal from water seems to be a more safe method than the use of photocatalyst powders directly dispersed in water.

As a consequence of the good result obtained after one hour under the UV-Vis lamp, the irradiation effect has been followed in time and the results are reported in the histogram of Fig.10.

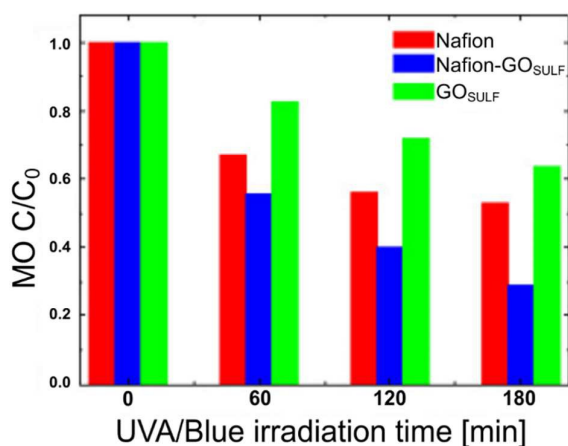


Fig.10: Residual concentration of MO versus time of contact with Nafion (red bar), Nafion- GO_{SULF} (blue bar) and GO_{SULF} (green bar) under UV/blue light irradiation.

Nafion-GO_{SULF} is able to remove about 70% of the initial MO concentration, after three hours. Comparing the degradation activity of GO_{SULF} powder with the relative nanocomposite, the reduction of MO concentration is much larger either in dark or under irradiation when the filler is embedded in the Nafion matrix. As just said, the irradiation favour MO degradation and in both case the polymer increases this degradation ability since it provides a larger number of active sites for MO absorption and this is also crucial for the photocatalytic process. In our previous work²⁴ a hypothesis of the possible photocatalytic mechanism for MO degradation by Nafion-GO_{SULF} was presented.

On the contrary, in the case of the cationic MB-dye, the powder itself works better than the composite membrane. This depends on the mutual interaction between the groups responsible of the adsorption (SO₃H) and the dye. Nevertheless, the dispersion of the material in the polymeric matrix has many advantages as above mentioned, in particular it is possible to reuse the same materials for successive purification processes. In our previous works²⁴⁻²⁵ we showed the possibility to reuse Nafion nanocomposites (with GO or TiO₂) after washing in water: after the first use, the membranes activity reduces but, then, it remains stable for the following cycles. The decreased efficiency after the first use could be due to a passivation of sulfonic groups that in the initial membrane preparation are activated by rinsing in acid media. Therefore, another regeneration process of the membranes was tested, by using 1% nitric acid in DI-water as described in the Experimental paragraph. In Fig. 11 we report MO and MB concentration for two consecutive uses of the same Nafion-GO_{SULF} membranes as adsorbent material in dark (a) or as photocatalytic material (b): fresh membrane in the first process and the regenerated membrane in the second one.

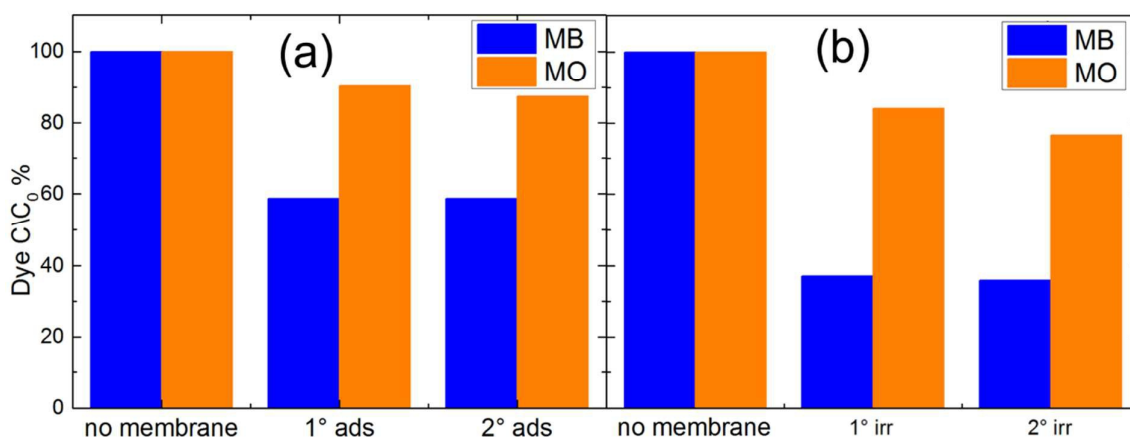


Fig.11: MO and MB residual concentration versus two consecutive (a) adsorption processes for 3 hours in dark or (b) photocatalytic processes for 3 hours, using the same pieces of Nafion-GO_{SULF} membrane. Between the first and the second process (adsorption or photocatalysis) the membranes were regenerated, as described in the text.

In the two cycles the performance of the membrane remains exactly the same, confirming the possibility of regeneration and reuse of these membranes without efficiency loss.

Conclusion

Graphene oxide functionalized by the introduction of sulfonic groups shows very good ability for the removal of dyes from water. In particular the material was tested directly dispersed in water or embedded in a polymeric matrix for the degradation of anionic and cationic dyes.

The presence of acid sulfonic groups on graphene oxide results in an increasing of cationic methylene blue-dye adsorption due to electrostatic interactions and with the appearance of methylene blue-organo modified graphene oxide (GO_{SULF}) precipitates. A slight increase of the degradation is observed after successive irradiation, while in graphene oxide, the irradiation after adsorption does not induce any extra methylene blue decrease.

The idea to incorporate such nanomaterials in a polymeric matrix is attractive to avoid the dispersion of powder in water and, in this work, Nafion polymer was tested as support matrix for photocatalysts. The results demonstrate that there is not any release of the powders in solution and that the nanocomposite membranes can be regenerated and reused.

In the case of a cationic dye, such as methylene blue, the role of the polymeric matrix is that of mechanical support for the nanomaterial avoiding its dispersion in the environment and allowing the reuse of the same amount of powder for successive purification processes. On the contrary, in the case of an anionic dye, such as methyl orange, the role of the Nafion is crucial for its interaction with the dye molecules, enhancing the degradation through a synergic effect of adsorption and photocatalytic reaction. For both dyes, the possibility of regeneration and reuse of these membranes after washing them in diluted (1%) acid solution is confirmed.

Acknowledgements

This research has been supported by the European Project WATER (Winning Applications of nanoTEchnology for Resolutive hydropurification), Grant Agreement 316082.

References

- 1 N. Savage, M. S.Diallo, *J Nanopart Res* , 2005, 7, 331–42.

- 2 D. F. Ollis, E. Pelizzetti, N. Serpone, In *Photocatalysis Fundamentals and Applications*, ed. N. Serpone, E. Pelizzetti, Wiley, New York, 1989, 18, 603.
- 3 D. F. Ollis, H. Al-Ekabi, *Photocatalytic Purification and Treatment of Water and Air*. Elsevier Science, Amsterdam, 1993.
- 4 M. R. Hoffmann, S. T. Martin, W. Choi, D. W. Bahnemann, *Chem Rev*, 1995, **95**, 69–96.
- 5 T. Sakata, T. Kawai, in *Energy Resources through Photochemistry and Catalysis*, ed. M. Gratzel, Elsevier, Amsterdam, 1983, 331–358.
- 6 H. Zollinger, *Properties of Organic Dyes and Pigments in Color Chemistry*, VCH Publishers, New York, 1978, 92–102.
- 7 T. Robinson, G. McMullan, R. Marchant, P. Nigam, *Bioresour Technol*, 2001, **77**, 247-255.
- 8 E. Forgacs, T. Cserháti, G. Oros, *Environ Int*, 2004, **30**, 953-971.
- 9 G. Crini, *Bioresour Technol*, 2006, **97**, 1061-1085.
- 10 M. Rafatullah, O. Sulaiman, R. Hashim, A. Ahmad, *J. Hazard. Mater.*, 2010, **177**, 70-80.
- 11 R. Andreatti, V. Caprio, A. Insola, R. Marotta, *Catal Today*, 1999, **53(1)**, 51–59.
- 12 M-Q Yang, N. Zhang, M. Pagliaro, Y-J Xu, *Chem. Soc. Rev.*, 2014, **43**, 8240.
- 13 N. Zhang, Y. Zhang, Y-J Xu *Nanoscale*, 2012, **4**, 5792.
- 14 X. Xie, K. Kretschmer, G. Wang, *Nanoscale*, 2015, **7**, 13278.
- 15 Y. Zhang, Z-R Tang, X. Fu, Y-J Xu, *ACS Nano*, 2010, **4(12)**, 7303-7314.
- 16 D. D'Angelo, C. Bongiorno, M. Amato, I. Deretzis, A. La Magna, G. Compagnini, S. F. Spanò, S. Scalese, *Carbon*, 2015, **93**, 1034-1041.
- 17 M-Q Yang, C. Han, N. Zhang, Y-J Xu, *Nanoscale*, 2015, **7**, 18062.
- 18 S.-T. Yang, S. Chen, Y. Chang, A. Cao, Y. Liu, H. Wang, *J Colloid Interface Sci*, 2011, **359**, 24–29.
- 19 T. F. Yeh, J. Cihlar, C. Y. Chang, C. Cheng, H. Teng, *Mater Today*, 2013, **16**, 78–84.
- 20 N. Zhang, M.Q. Yang, S. Liu, Y. Sung, Y.J. Xu, *Chem. Rev.*, 2015, **115 (18)**, 10307–10377
- 21 N. Zhang, Y.J. Xu, *Cryst Eng Comm*, 2016, **18**, 24 – 37.
- 22 S. Filice, D. D'Angelo, S. F. Spanò, G. Compagnini, M. Sinatra, L. D'Urso, E. Fazio, V. Privitera, S. Scalese, *Mater Sci Semicond Proc*, 2015, **42**, 50-53.
- 23 N. Oger, Y. F. Lin, C. Labrugere, E. Le Grogneec, F. Rataboul, F.-X. Felpin, *Carbon*, 2016, **96**, 342-350.
- 24 S. Filice, D. D'Angelo, S. Libertino, I. Nicotera, V. Kosma, V. Privitera, S. Scalese, *Carbon*, 2015, **82**, 489-499.
- 25 D. D'Angelo, S. Filice, S. Libertino, V. Kosma, I. Nicotera, V. Privitera, S. Scalese,

Photocatalytic Properties of Nafion Membranes Containing Graphene Oxide/Titania Nanocomposites, presented at IEEE 9th Nanotechnology Materials and Devices Conference (NMDC) 2014, Acicastello (Catania), October, 2014.

26 A. Enotiadis, K. Angjeli, N. Baldino, I. Nicotera, D. Gournis, *Small*, 2012, **8**, 3338–3349.

27 C. Heitner-Wirguin, *J Membr Sci*, 1996, **120**, 1–33.

28 S. J. Sondheimer, N. J. Bunce, M. E. Lemke, C. A. Fyfe, *Macromolecules*, 1986, **19**, 339–343.

29 Y. Shen, B. Chen, *Environ Sci Technol*, 2015, **49** (12), 7364–7372.

30 L. Staudenmaier, *Ber Dtsch Chem. Ges.*, 1899, **31**, 1481–1487.

31 Y. Shen, B. Chen, *Environ. Sci. Technol.*, 2015, **49** (12), 7364–7372.

32 N. Liaros, J. Tucek, K. Dimos, A. Bakandritsos, K.S. Andrikopoulos, D. Gournis, R. Zboril and S. Couris, *Nanoscale* 2016, **8**, 2908–2917.

33 K. Dimos, I. Panagiotopoulos, T. Tsoufis, R.Y.N. Gengler, A. Moukarika, P. Rudolf, M.A. Karakassides, T. Bakas and D. Gournis, *Langmuir* 2012, **28**, 10289–10295.

34 M. M. Nasef, H. Saidi, H. M. Nor, M. A. Yarmo, *J. Appl. Polym. Sci.* 2000, **76**, 336–349.

35 K. S. Siow, L. Britcher, S. Kumar, H. J. Griesser, *Plasma Process. Polym.* 2009, **6**, 583–592.

36 P. Montes-Navajas, N. G. Asenjo, R. Santamaría, R. Menéndez, A. Corma, H. García, *Langmuir*, 2013, **29**, 13443–13448.

37 A. M. Mika, K. Lorenz, A. Szczurek, *J Membr Sci*, 1989, **41**(15), 163–176.

38 A. R. Khataee, M. B. Kasiri, *J Mol Catal A: Chem*, 2010, **328**, 8–26.

39 I. Nicotera, C. Simari, L. Coppola, P. Zygouri, D. Gournis, S. Brutti, F. D. Minuto, A. S. Aricò, D. Sebastian, V. Baglio, *J Phys Chem C*, 2014, **118**, 24357–24368.

40 H. Park, W. Choi, *J Phys Chem B*, 2005, **109**, 11667–11674.

41 W. C. Yen, H. C. Lin, J. S. Huang, Y. J. Huang, Y. L. Chueh, *Sci Adv Mater*, 2014, **6**, 1–8.

42 S. Al-Qaradawi, S. R. Salman, *J Photochem Photobiol A*, 2002, **148**, 161–168.

43 H. Trabelsi, M. Khadhraoui, O. Hentati, M. Ksibi, *Toxicol Environ Chem*, 2013, **95**, 543–558.

Figure captions

Fig.1: Schematic representation of the structures of GO (top) and GO_{SULF} nanoplatelets (bottom).

Fig.2: Structure of methyl orange (left) and methylene blue (right).

Fig. 3: X-ray photoemission spectra of (a) C1s core level for starting GO and (b) C1s, (c) S2p and (d) N1s for sulfonated GO.

Fig. 4: Cross-sectional SEM images of (a) Nafion membrane and (b) Nafion-GO_{SULF} membrane loaded with 3% of GO_{SULF}; (c) GO_{SULF} powder dispersed on a Si substrate.

Fig. 5: (a) UV–Vis absorbance spectra of MB solution after adding GO_{SULF} powder with different concentrations: 10 mg/l (green curve) 70 mg/l (blue curve) and 100 mg/l (red curve). The initial absorbance of the MB is also reported (black curve). The photo in the inset shows the beakers containing the MB solutions with GO_{SULF} with increasing concentration (from left to the right). In (b) and (c) the removed MB (%) as a function of GO_{SULF} concentration or as a function of the [MB]/[GO_{SULF}] concentration ratio are reported, respectively. The lines in the plots are just a guide for the eye.

Fig.6: MB residual concentration versus time of contact with GO and GO_{SULF} powders (both with a concentration of 70 mg/l). The UV-blue lamp irradiation starts after 30 min of adsorption in dark, as indicated by the vertical line at $t = 0$ min. Lines in figure are guides for the eyes. The photos in the inset show the beakers containing the MB solutions with GO_{SULF} and GO after 10 min adsorption ($t = -20$)

Fig.7: MB residual concentration versus time of contact with Nafion and Nafion-GO_{SULF} in dark (red and blue dots, respectively) and under irradiation (magenta and cyan dots, respectively).

Fig.8: MB residual concentration versus contact time in dark with Nafion-GO_{SULF} membranes having different surface areas. In the inset we report the pictures of the membranes used for MB adsorption (from left to right: 0.25 cm², 0.5 cm², 1 cm²) and the cuvettes with initial MB solution (first on the left) and solutions after dipping the three Nafion-GO_{SULF} membranes for 5 hours.

Fig.9: UV–Vis absorbance spectra of methyl orange after immersing Nafion (red curves), Nafion-GO_{SULF} (blue curves) composite membranes and GO_{SULF} powder (green curves) in MO solution for one hour in dark (a) or under UV/blue irradiation (b).

Fig.10: Residual concentration of MO versus time of contact with Nafion (red bar), Nafion-GO_{SULF} (blue bar) and GO_{SULF} (green bar) under UV/blue light irradiation.

Fig.11: MO and MB residual concentration versus two consecutive (a) adsorption processes for 3 hours in dark or (b) photocatalytic processes for 3 hours, using the same pieces of Nafion-GO_{SULF} membrane. Between the first and the second process (adsorption or photocatalysis) the membranes were regenerated, as described in the text.

Graphical abstract

Use of graphene oxide flakes functionalized with 3-amino-1-propanesulfonic acid (GO_{SULF}), as powder or incorporated into a Nafion membrane, for the removal of cationic and anionic dyes is studied.

